THE JOURNAL OF PHYSICAL CHEMISTRY Letters

Letter

Cite This: J. Phys. Chem. Lett. 2017, 8, 5593-5598

pubs.acs.org/JPCL

Size-Dependent Level Alignment between Rutile and Anatase TiO_2 Nanoparticles: Implications for Photocatalysis

Kyoung Chul Ko,[†,‡] Stefan T. Bromley,*[,†,§] Jin Yong Lee,*[,‡] and Francesc Illas[†]

[†]Departament de Ciència de Materials i Química Física & Institut de Química Teòrica i Computacional (IQTCUB), Universitat de Barcelona, C/Martí i Franquès 1, 08028 Barcelona, Spain

[‡]Department of Chemistry, Sungkyunkwan University, Suwon 16419, Korea

[§]Institució Catalana de Recerca i Estudis Avançats (ICREA), 08010 Barcelona, Spain

Supporting Information

ABSTRACT: Motivated by the enormous importance of nanoscale TiO_2 in a wide range of photocatalytic applications and the ill-understood high activity of the commercial nano-TiO_2 photocatalysts, we provide a predictive map of how the anatase−rutile level alignment varies from the smallest nanoparticles (NPs) to the bulk. Specifically, we compute the size dependence of the energies of vacuum-referenced electronic levels in a range of realistically structured rutile and anatase TiO_2 NPs employing accurate all-electron density functional calculations. In agreement with most recent work, a staggered type II anatase level alignment is predicted for the bulk phases, which we further find to persist into the regime of large NPs. We predict that other level alignments will emerge when the diameter of the TiO_2 NPs is reduced below ∼15 nm. Our results suggest how experiment could test the widely debated importance of the bulk-like type II anatase level alignment for enhanced photoactivity of nano-TiO_2.

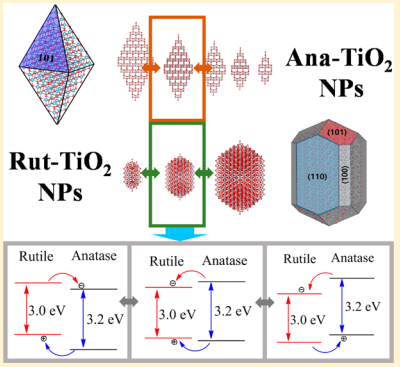

The energy mismatch between electronic levels belonging, respectively, to two distinct chemical/material systems when interfaced (e.g., inorganic−inorganic,[1] metal−organic,[2] defect−host[3]) is a key measure controlling intersystem charge transfer. The degree of such level alignment can, in turn, affect a range of important properties such as photocatalysis and conduction. Level alignment can also be deliberately engineered to improve the performance of technological applications (e.g., solar cells[4]). The high activity of the commercial Degussa P25 titania (TiO_2) ultraviolet (UV) photocatalyst is also often attributed to the way in which the electronic levels in the constituent anatase and rutile nanophases are aligned at their interfaces.[5] Sophisticated experiments using surface-sensitive techniques have related the high photocatalytic activity of some TiO_2 samples to the surface-phase structure and reported enhanced activity when anatase TiO_2 nanoparticles are highly dispersed on the surface of rutile TiO_2.[6] In these cases anatase−rutile level alignment has been proposed as the main factor for determining separation of the photogenerated free charge carriers,[7] which potentially provides a means to optimize TiO_2 for applications such as hydrogen production from water splitting.[8] Despite concerns raised by some authors about the role of nanoparticulate anatase−rutile interactions in determining the photocatalytic activity of mixed titania phases,[9,10] considerable work has been devoted to determining the type of level alignment at anatase−rutile interfaces from both experiment and theory (see ref 1 and references therein). As yet, however, there is no general consensus for this important system and the three general possibilities proposed in the literature are summarized in Figure 1.[11] Two other reported

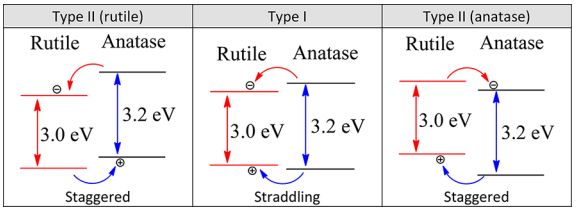

Figure 1. Schematic diagram showing possible anatase−rutile level alignments of the HOMO and LUMO for each respective phase, with arrows indicating associated charge transfer possibilities.

scenarios where either the valence or the conduction bands in the two respective phases are perfectly aligned[12] can be regarded as special cases of the three main alignment types.

The origin of the discrepancies between different studies, with regard to the experimentally reported anatase−rutile level alignment type, appears to derive largely from the use of different titania samples. This issue is particularly acute in the case of nanoparticles prepared by different experimental techniques, where reproducibility is challenging with respect to numerous properties (e.g., surface effects, shape, and size). Computational modeling approaches to evaluating the electronic structure, although inherently more reproducible, are also not free of problems. Periodic models of crystals and surfaces, for example, intrinsically lack an absolute energy

Received: September 18, 2017
Accepted: October 23, 2017
Published: October 23, 2017

DOI: 10.1021/acs.jpclett.7b02474
J. Phys. Chem. Lett. 2017, 8, 5593−5598

reference for the electronic levels, thus requiring the modeler to define a common energy for each separate calculation. Despite such issues, recent analysis of reported results concluded that the staggered type II (anatase) level alignment (see Figure 1) is most appropriate for describing bulk anatase−rutile interfaces.[11] We note that this conclusion is in agreement with the perhaps most convincing study yet reported resulting from the combined use of quantum mechanical/molecular mechanical (QM/MM) embedding modeling and X-ray photoelectron spectroscopy.[1] Recently, it was theoretically predicted that subtle changes of the contact interfacial region including types of TiO_2 surface facets[13] and/or adsorbed ionic effects[14] could affect level alignment. Nonetheless, most periodic DFT calculations for mixed-phase bulk TiO_2 without defect states[15,16] or with defect states[17,18] support the staggered type II (anatase) alignment. Although the situation regarding bulk anatase−rutile interfaces appears to be approaching a consensus, it is known from experiment[5,19] and theory[20,21] that titania nanoparticle size has significant influence on the electronic structure, which is likely to affect the level alignment at nanoscale anatase−rutile interfaces. The majority of photocatalytic applications of titania rely on nanostructured or nanoparticulate samples, where both anatase and rutile polymorphs are likely to occur together. However, fundamental and technologically important questions regarding the anatase−rutile level alignment in such nano-TiO_2 systems remain open.

Herein, following previous works,[20,21] we investigate how the level alignment between anatase and rutile nanoparticles depends on their size using all-electron, relativistic, density functional theory (DFT)-based calculations using the FHI-AIMS[22] code. We note that our approach, as with QM/MM calculations, has the advantage over periodic models that it allows one to compute all energy levels of interest referred to the vacuum level without further additional assumptions. Anatase nanoparticles with an octahedral structure exhibiting the most stable (101) surface following the Wulff construction[23] were considered, as in previous work.[20,21] The resulting nanoparticles are denoted as a-$(TiO_2)_n$ with n = 35, 84, 165, 286, and 455. In the case of rutile r-$(TiO_2)_n$ nanoparticles, two different nanoparticle groups have been considered depending on whether they follow or not the Wulff construction. Rutile nanoparticles with n = 51, 211, and 563 correspond to Wulff cuts exhibiting (110), (101), and (001) facets. However, r-$(TiO_2)_n$ nanoparticles for n = 86 and 111 were obtained by further truncating the (211) facets along the longest axis and are thus quasi-Wulff with shapes that do not mirror those typically found in experiment. These quasi-Wulff nanoparticles are found to be energetically metastable with respect to Wulff-constructed r-$(TiO_2)_n$ nanoparticles and not thus employed in our level alignment analysis. For both anatase and rutile, the nanoparticles are of a size that can be considered to be in the scalable regime where properties scale linearly with inverse particle size.[24] The shapes of the Wulff-like nanoparticles employed are shown in Figure 2. Our designed nanoparticles following the Wulff construction represent thermodynamic equilibrium shapes for individual isolated anatase and rutile nanoparticles. From the calculated electronic structure of the nanoparticles, we can estimate how the alignment of the electronic levels between the two nanoparticle types varies according to independent changes of anatase and rutile nanoparticle size. Diameters are taken to be the largest vertex-to-vertex distance through the respective nanoparticle (see Figure 2). The atomic structure of all nanoparticles was

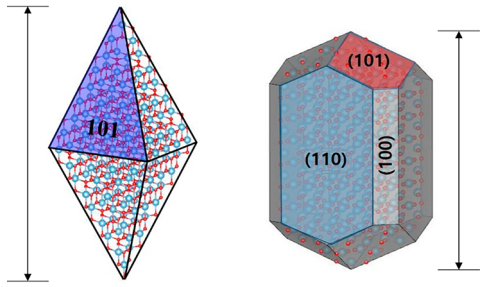

Figure 2. Wulff-type anatase (left) and rutile (right) nanoparticle morphologies. Anatase nanoparticles a-$(TiO_2)_n$ with sizes n = 35, 84, 165, 286 and 455 and rutile nanoparticles r-$(TiO_2)_n$ nanoparticles with n = 51, 211, and 563 were employed for the level alignment calculations. Arrows indicate the maximum vertex−vertex distance in each case, which we take to be the corresponding nanoparticle diameter.

first optimized at the DFT level using the Perdew−Bruke−Ernzerhof[25] (PBE) functional and a light/tier 1 numerical atom-centred orbital basis set (see ref 21 and Supporting Information for all optimized nanoparticle structures). The electronic structure of all PBE-optimized nanoparticles was subsequently obtained using the hybrid PBEx functional containing 12.5% nonlocal Fock exchange. This percentage of exchange was derived in previous work as to reproduce the band gap of both reduced and stoichiometric bulk anatase and rutile.[26] We note that for the largest r-$(TiO_2)_{563}$ nanoparticle, direct PBEx calculations were computationally intractable and the Kohn−Sham orbital energies were estimated from a linear relation between PBE and PBEx Kohn−Sham electronic levels (see Supporting Information).

Due to their finite relatively small size, the electronic levels in $(TiO_2)_n$ nanoparticles are susceptible to quantum confinement effects. Rudimentary particle-in-a-box models predict a general $n^{-2/3}$ size dependence of nanoparticle electronic energy levels. This can be understood by noting that the energy (E) of any electronic level in the particle-in-a-box model has the relation $E \propto L^{-2}$, where L is the length of the box. For a nanoparticle, L becomes the nanoparticle diameter. If we set the density of nanoparticle as n/V (where n is the number of formula units and V is volume), because V is proportional to L^3 for a fixed density, the relation $n \propto L^3$ holds. From the relations $E \propto L^{-2}$ and $n \propto L^3$, E is thus proportional to $n^{-2/3}$. It is known that such models are overly simplified as they do not take into account factors such as the atomic structure or surface stresses on the electronic structure. An improved fitting of the size dependency of energy levels obtained from experiment[27] or realistic quantum mechanical modeling[28] can often be found using $n^{-\alpha/3}$, where $1 < \alpha < 2$. In line with previous work on InP nanoparticles,[28,29] we find α = 1.35 to be a suitable choice for fitting our size-dependent energy level data.

Figure 3 shows the dependence of the highest occupied molecular orbital (HOMO) and the lowest unoccupied molecular orbital (LUMO) energy levels obtained at the PBEx level of theory for both a-$(TiO_2)_n$ and r-$(TiO_2)_n$ with respect to $n^{-1.35/3}$. For the a-$(TiO_2)_n$ nanoparticles, with increasing size, the energies of the HOMO and LUMO levels tend to slowly converge towards each other, meaning that the $E_{LUMO}-E_{HOMO}$ energy gap ($E_{[LUMO-HOMO]}$) decreases with increasing size and *vice versa* (see Figure 4). This behavior is as expected from simple quantum confinement arguments.[29] For a-$(TiO_2)_n$ nanoparticles for n = 35−455, the character of the

DOI: 10.1021/acs.jpclett.7b02474
J. Phys. Chem. Lett. 2017, 8, 5593−5598

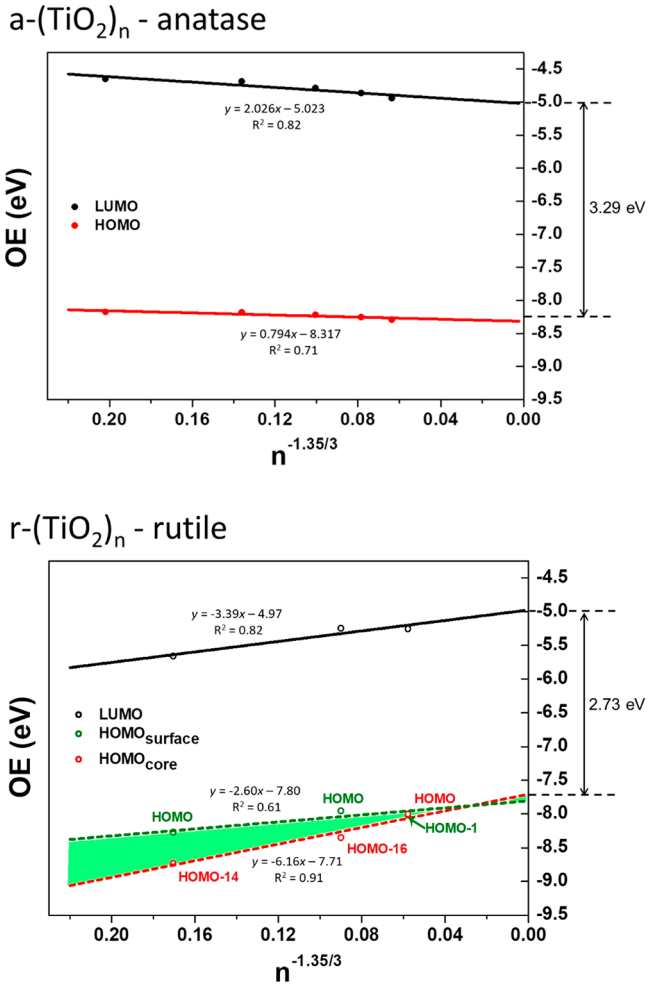

Figure 3. Variation of the PBEx-calculated HOMO and LUMO orbital energies (OE in eV) of a-$(TiO_2)_n$ (upper) and r-$(TiO_2)_n$ (lower) nanoparticles as a function of $n^{-1.35/3}$. To the right of each plot the respective extrapolated bulk band gap is shown.

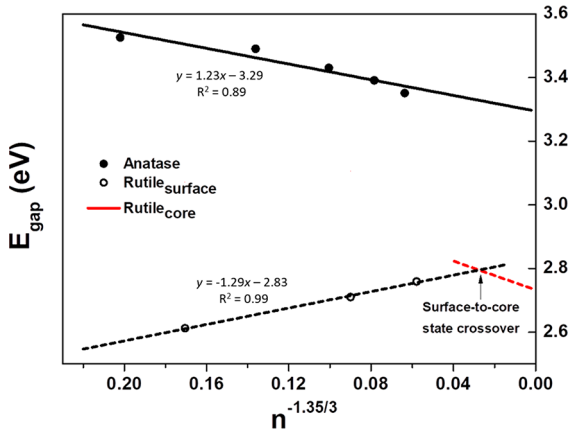

Figure 4. Variation of the PBEx-calculated $E_{HOMO-LUMO}$ gap (eV) of a-$(TiO_2)_n$ and r-$(TiO_2)_n$ nanoparticles as a function of $n^{-1.35/3}$. The $Rutile_{core}$ line is derived from the difference between LUMO and $HOMO_{core}$ fits in Figure 3.

HOMO and LUMO is found to be similar, showing in each case an electronic distribution mainly on the central core parts of the nanoparticles. For the largest a-$(TiO_2)_{455}$ nanoparticle, we note that the LUMO maintains its core state character but with some electronic density slightly shifted toward the surface.

In contrast, for rutile nanoparticles (Figure 3, lower), the HOMO and LUMO values tend to diverge from each other with increasing size. In other words, smaller nanoparticles have a smaller energy gap, indicating an inverse quantum confinement trend. Previous studies in the literature have reported that, in small finite systems, such an inverse quantum confinement tendency can be associated with the interference of localized surface states on frontier orbital states.[30,30] For instance, cases with $E_{HOMO(core)} < E_{HOMO(surface)}$ and/or $E_{LUMO(core)} > E_{LUMO(surface)}$ would have surface states as frontier orbitals instead of a core states, with a concomitant effect on the magnitude of the frontier orbital energy gap. We find that the HOMO level and a number of energetically close occupied levels for the r-$(TiO_2)_{51,211}$ rutile nanoparticles have a strong surface state character with a significant orbital contribution on dangling oxygen atoms or exposed surface atoms (see Figure S6 in the Supporting Information).

In an ideal bulk crystal, the frontier energy levels would correspond to core (bulk-like) states constituting the valence and conduction bands, and localized surface states are formally excluded. In this regard, we should expect that the HOMO of the r-$(TiO_2)_n$ nanoparticles will gradually become less surface-like and more core-like with increasing size, eventually forming a bulk-like state in the limiting case of infinite particles. In order to estimate the size at which this state crossover occurs for each r-$(TiO_2)_n$ nanoparticle, we systematically searched the energy levels below the HOMO for the highest energy state that exhibits primarily core-like characteristics and did not contain significant orbital contribution on dangling oxygens and exposed surface atoms (see Figure S6 in the Supporting Information). For the r-$(TiO_2)_{51}$ and r-$(TiO_2)_{211}$ nanoparticles, these HOMO(core) levels were found for HOMO−14 and HOMO−16 levels (where HOMO-*a* corresponds to the *a*th electronic level below the HOMO), respectively. On the other hand, for the largest r-$(TiO_2)_{563}$ nanoparticle, HOMO and HOMO−1 states, which are energetically very close, can be classified as HOMO(core) and HOMO(surface) states, respectively. Thus, the size of the r-$(TiO_2)_{563}$ nanoparticle is close to that where the HOMO characteristics change from being surface-like to core-like with increasing nanoparticle size (see the Supporting Information). Consequently, regular quantum confinement trends are expected for energy gaps between HOMO(core) and LUMO states, for rutile nanoparticles of size r-$(TiO_2)_{563}$ and larger (see the red line in Figure 4).

To confirm the consistency of our nanoparticle calculations with calculated band gaps from periodic bulk calculations, we extrapolate the linear fits of the E_{HOMO} and E_{LUMO} values for each nanoparticle type as a function of $n^{-1.35/3}$ to the bulk (i.e., $n^{-1.35/3} \rightarrow 0$) and extract E_{gap} values for each titania polymorph (see the Supporting Information for fitting details). From this procedure, we obtain bulk band gap estimates of 3.24 eV for anatase and 2.73 eV for rutile. These extrapolated values differ by only +0.05 and −0.18 eV, respectively, relative to anatase and rutile band gaps obtained from periodic calculations using the same PBEx functional, giving us confidence in our bottom-up approach.[26] For rutile, the slightly larger difference between the extrapolated $E_{[LUMO-HOMO(core)]}$ value and the periodic E_{gap} value may be due to the relative uncertainty associated with the manual identification of suitable HOMO(core) states required for making extrapolation to the bulk. We also note that the bulk

DOI: 10.1021/acs.jpclett.7b02474
J. Phys. Chem. Lett. 2017, 8, 5593−5598

extrapolated nanoparticle LUMO values for anatase (−5.02 eV) and rutile (−4.97 eV) are found also to compare very well with reported experimental values of 5.1 and 4.9 eV, respectively.[31] Although it is important that our nanoparticle data can be extrapolated to yield consistent and reasonably accurate bulk values, the main advantage of our bottom-up approach is that it permits us to follow the size dependency of the rutile−anatase level alignment. In Figure 5, we plot a color-shaded plot of

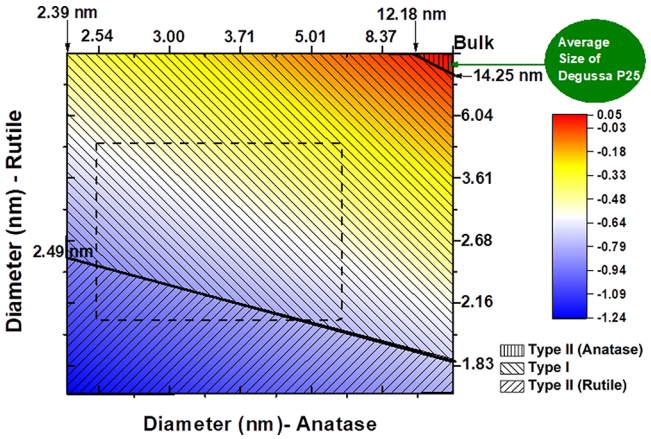

Figure 5. Map of level alignment as a function of the independent size variation of anatase and rutile phases. Types of level alignment are divided in three regions having different respective patternings. The green arrow points to the location on the map where the sizes of anatase and rutile nanoparticles approximately correspond to those found in Degussa P25. The square marked by dashed lines denotes the limits of the nanoparticle size region explicitly studied in the present work. The gradation of color relates to the r-LUMO − a-LUMO energy difference (eV), which provides an estimate of the electron transfer tendencies between the two respective rutlile and anatase phases (see Figure 1). We note that the *x*-axes in the plots in Figures 3 and 4 correspond to following an $x = y$ line through the level alignment map.

$E_{\text{r-LUMO}}-E_{\text{a-LUMO}}$ with respect to nanoparticle size for rutile and anatase separately. In Figure 5, the associated estimated nanoparticle diameters are derived using the correlations plotted in Figure S7 (see Supporting Information), and the regions corresponding to different types of level alignment (see Figure 1) are indicated by different shading patterns.

For the bulk limit (top right corner of Figure 5), the extrapolated fits predict a staggered type II (anatase) rutile−anatase level alignment consistent with the type of bulk rutile−anatase level alignment largely predicted by experiment and theory.[1,11] Specifically, we obtain a difference of 0.61 eV between the energies of the respective valence band maxima (VBM) and a difference of 0.05 eV between the energies of the respective conduction band minima (CBM). These differences are also in reasonable agreement with the respective differences of ∼0.4 and 0.2 eV found in ref 1. In addition, we predict that type II (anatase) level alignment will be persistent in a size range covering the bulk to moderately sized nanoparticles. Specifically, if we follow size reduction from the bulk by varying $n^{-1.35/3}$ for both types of nanoparticle simultaneously, as in Figure 3, we find a crossover to a straddling type I level alignment at $n^{-1.35/3} = 0.00825$ where the rutile E_{LUMO} becomes lower than that of anatase. This crossover occurs at an anatase nanoparticle diameter of 26.9 nm and a rutile nanoparticle diameter of 19.4 nm. In Figure 5, we further show how this crossover varies with respect to independent changes in the size of both anatase and rutile nanoparticles. This representation shows us that the smallest nanoparticle diameters for which type II (anatase) level alignment is predicted to be maintained is ∼14 nm for anatase (with respect to bulk rutile) and ∼12 nm for rutile (with respect to bulk anatase). We note that the average diameters of anatase and rutile nanoparticles in Degussa P25 have been reported to be 85 and 25 nm, respectively.[5,10] In Figure 5, this situation corresponds to the point on the map indicated by a green arrow, which is located well within the region of type II (anatase) level alignment.

That the crossover between type II (anatase) and type I level alignment is predicted to occur at nanoparticle diameters of ∼10−15 nm has practical implications for both theory and experiment. First, this size regime is beyond the current tractable size for computational methods that can provide a reasonably accurate description of the electronic structure of TiO_2 (e.g., DFT using PBEx). We would thus expect that all suitably accurate modeling of discrete nanoparticles to predict either type I or a staggered type II (rutile) level alignment. We predict that type II (rutile) level alignment would occur only when rutile nanoparticles become smaller than 2−2.5 nm diameter (see lower region in Figure 5). We note that surface passivation of TiO_2 nanoparticles can prevent the surface-like character of the HOMO and LUMO and thus may allow core-like electronic states at relatively smaller sizes than the bare nanoparticles studied herein. Kang et al. performed a theoretical study of this type with pseudohydrogen-terminated nanoparticles of anatase and rutile containing 110−130 atoms and found the type I level alignment with aligned valence bands (i.e., at the crossover between type II (rutile) and type I).[32] This suggests that even with passivation direct modeling of rutile and anatase nanoparticles of a sufficient size to exhibit type II (anatase) level alignment will remain intractable. Our direct modeling of a set of well-defined bulk-cut anatase and rutile nanoparticles with diameters between 2 and ∼6 nm using an accurate DFT-based approach uniquely allows us to make vacuum-referenced extrapolations to the crossover size regime between type II (anatase) and type I level alignment. In Figure 5, the rectangular region marked by dashed lines indicates the size range explicitly covered by our calculations.

Our predictions also have potential practical experimental implications. Although our extrapolations inevitably have some associated uncertainties, they clearly show that there are finite nanoparticle size regimes of stability for the type II (anatase), type I, and type II (rutile) level alignments. For type II (rutile) level alignment (see Figure 1), our results imply that at least one of the nanoparticles should have a diameter of <2.5 nm (see Figure 5). Recent work, however, has predicted that bare TiO_2 nanoparticles in this size regime are energetically more stable when noncrystalline.[20] Thus, any such small rutile or anatase nanoparticles will likely be at best metastable and/or spontaneously relax to a distorted nonordered structure causing a significant change in electronic structure, likely disturbing the type II (rutile) level alignment. This strongly suggests that experimental realization of type II (rutile) level alignment in a rutile−anatase system would be difficult to achieve.

Our calculations also imply that the smallest diameter of anatase nanoparticle that can yield type II (anatase) level alignment is ∼14 nm (see Figure 5). The crossover size predicted for the thermodynamic stability of bare anatase versus rutile nanoparticles is also predicted to be at a diameter of ∼14 nm.[33] This formally implies that in order to achieve the type II

DOI: 10.1021/acs.jpclett.7b02474
J. Phys. Chem. Lett. 2017, 8, 5593−5598

(anatase) level alignment using bare nanoparticles thermodynamically metastable anatase nanoparticles (i.e with diameters > 14 nm) would be required. In experimental samples, interaction of TiO_2 nanoparticle surfaces with their environment (e.g., variable pH, hydroxylation) can typically shift the bare anatase−rutile thermodynamic crossover size upward by 5−15 nm,[34] which is likely to play a role in the stabilization of larger anatase nanoparticles for promoting type II (anatase) level alignment. We note that in Degussa P25 the anatase nanoparticles are rather large (85 nm diameter), which we would expect to strongly promote a type II (anatase) band alignment. This type of level alignment implies that the LUMO of the rutile phase is higher in energy than the LUMO of the anatase phase, which suggests that transfer of excited electrons in rutile to the LUMO of active anatase could be facilitated. Similarly, the higher energy of the rutile HOMO relative to that of anatase in such a level alignment could help promote the accumulation of holes in the rutile phase. The estimated electron and hole transfer tendencies according to the diameter of anatase and rutile phases are displayed by the gradations of color in Figure 5 and also in Figure S8, respectively. Overall, these charge transfers could also lead to charge separation on the two separate phases (i.e., holes on rutile, electrons on anatase; see Figure 1), perhaps synergistically promoting anatase-based photochemistry, as claimed by some authors (see refs 35 and 36 and references therein). Conversely, in a type I level alignment, both electron and hole transfer to the rutile phase would be more energetically favored, leading to more likely electron−hole recombination and a significantly lower photoactivity (see Figure 1). Our results imply that these scenarios could both be accessed through controlling the size of either (or both) of the constituent nanoparticles. Following the above, if level alignment plays such a crucial role in the performance of rutile−anatase nanoparticle-based catalysts, we would expect to see a significant shift in the photoactivity of such systems when either the rutile or anatase (or both) nanoparticles become smaller than a critical size. Our results for bare nanoparticles suggest a critical crossover size for type II (anatase) to type I level alignment to occur for diameters close to 14 nm. In experimental setups where the nanoparticle surfaces could interact with adsorbates (e.g., water), this size could be somewhat higher.

To summarize, using all-electron, relativistic DFT-based calculations with a suitably tailored hybrid functional, we have modeled a set of realistic rutile and anatase nanoparticles. On the basis of the size-dependent variation in the electronic structure of these nanoparticles, we have extrapolated the vacuum-referenced energy levels from the nanoscale to the bulk limit. The thus extracted type II (anatase) bulk band alignment is in full agreement with the most recent estimates from a variety of experimental and theoretical techniques.[1,11] Due to our accurate bottom-up approach, we are thus uniquely able to calculate how the level alignment between anatase and rutile depends on size. Our analysis clearly shows that the level alignment can vary among (i) type II (anatase) for bulk and larger nanoparticles, (ii) type I when at least one nanoparticle type has a diameter less than ∼15 nm, and (iii) type II (rutile) when at least one nanoparticle has a diameter less than ∼2.5 nm. The potential implications of our results for both theoretical modeling and experiment are also discussed. In particular, we propose that the suggested importance of the bulk-like type II (anatase) level alignment for enhanced photoactivity could be experimentally tested via control of nanoparticle size to shift to a type I level alignment.

■ ASSOCIATED CONTENT

Supporting Information

The Supporting Information is available free of charge on the ACS Publications website at DOI: 10.1021/acs.jpclett.7b02474.

Nanoparticle models, computational details, calculated SCF energies for quasi-Wulff type rutile nanoparticles, r-$(TiO_2)_{86}$ and r-$(TiO_2)_{111}$, estimate of the PBEx orbital energies (OE in eV) for r-$(TiO_2)_{563}$, calculated molecular orbitals and their corresponding energy levels (in eV), relationship between the diameter of nanoparticles and $n^{1/3}$, PBE- and PBEx-calculated molecular energy levels and energy per unit (in eV), and additional references (PDF)

■ AUTHOR INFORMATION

Corresponding Authors

*E-mail: s.bromley@ub.edu (S.T.B.).
*E-mail: jinylee@skku.edu (J.Y.L.).

ORCID

Kyoung Chul Ko: 0000-0003-4386-9112
Stefan T. Bromley: 0000-0002-7037-0475
Jin Yong Lee: 0000-0003-0360-5059
Francesc Illas: 0000-0003-2104-6123

Notes

The authors declare no competing financial interest.

■ ACKNOWLEDGMENTS

This research was supported by the Spanish MINECO/AEI-FEDER grant CTQ2015-64618-R and, in part, by Generalitat de Catalunya grants 2014SGR97 and XRQTC. The research in this work is in the framework of the NOMAD Center of Excellence project, which received funding from the European Union's Horizon 2020 research and innovation programme under Grant Agreement No. 676580. Computational time at the Marenostrum supercomputer of the Barcelona Supercomputing Center was provided through grants from the Red Española de Supercomputación. K.C.K. acknowledges financial support by the Basic Science Research Program through the National Research Foundation of Korea (NRF) funded by the Ministry of Education (NRF-2016R1A6A3A11933303) and support from the KISTI supercomputing center through the strategic support program for the supercomputing application research No. KSC-2016-C3-0046. F.I. acknowledges additional support from the 2015 ICREA Academia Award for Excellence in University Research.

■ REFERENCES

(1) Scanlon, D. O.; Dunnill, C. W.; Buckeridge, J.; Shevlin, S. A.; Logsdail, A. J.; Woodley, S. M.; Catlow, C. R. A.; Powell, M. J.; Palgrave, R. G.; Parkin, I. P.; Watson, G. W.; Keal, T. W.; Sherwood, P.; Walsh, A.; Sokol, A. Band Alignment of Rutile and Anatase TiO_2. *Nat. Mater.* **2013**, *12*, 798−801.

(2) Ishii, H.; Sugiyama, K.; Ito, E.; Seki, K. Energy Level Alignment and Interfacial Electronic Structures at Organic/Metal and Organic/Organic Interfaces. *Adv. Mater.* **1999**, *11*, 605−625.

(3) Van de Walle, C. G.; Neugebauer, J. Universal Alignment of Hydrogen Levels in Semiconductors, Insulators and Solutions. *Nature* **2003**, *423*, 626−628.

DOI: 10.1021/acs.jpclett.7b02474
J. Phys. Chem. Lett. 2017, 8, 5593−5598

(4) Chuang, C.-H. M.; Brown, P. R.; Bulović, V.; Bawendi, M. G. Improved Performance and Stability in Quantum Dot Solar Cells Through Band Alignment engineering. *Nat. Mater.* **2014**, *13*, 796−801.
(5) Ohno, T.; Sarukawa, K.; Tokieda, K.; Matsumura, M. Morphology of a TiO_2 Photocatalyst (Degussa, P-25) Consisting of Anatase and Rutile Crystalline Phases. *J. Catal.* **2001**, *203*, 82−86.
(6) Zhang, J.; Xu, Q.; Feng, Z.; Li, M.; Li, C. Importance of the Relationship between Surface Phases and Photocatalytic Activity of TiO_2. *Angew. Chem., Int. Ed.* **2008**, *47*, 1766−1769.
(7) Li, G.; Gray, K. A. The Solid−Solid Interface: Explaining the High and Unique Photocatalytic Reactivity of TiO_2-based Nanocomposite Materials. *Chem. Phys.* **2007**, *339*, 173−187.
(8) Fujishima, A.; Honda, K. Electrochemical Photolysis of Water at a Semiconductor Electrode. *Nature* **1972**, *238*, 37−38.
(9) Ohtani, B.; Prieto-Mahaney, O.; Li, D.; Abe, R. What is Degussa (Evonik) P25? Crystalline Composition Analysis, Reconstruction from Isolated Pure Particles and Photocatalytic Activity. *J. Photochem. Photobiol., A* **2010**, *216*, 179−182.
(10) Habisreutinger, S. N.; Schmidt-Mende, l.; Stolarczyk, J. K. Photocatalytic Reduction of CO_2 on TiO_2 and Other Semiconductors. *Angew. Chem., Int. Ed.* **2013**, *52*, 7372−7408.
(11) Nosaka, Y.; Nosaka, A. Y. Reconsideration of Intrinsic Band Alignments within Anatase and Rutile TiO_2. *J. Phys. Chem. Lett.* **2016**, *7*, 431−434.
(12) Mi, Y.; Weng, Y. Band Alignment and Controllable Electron Migration between Rutile and Anatase TiO_2. *Sci. Rep.* **2015**, *5*, 11482.
(13) Li, W.-K.; Hu, P.; Lu, G.; Gong, X.-Q. Density Functional Theory Study of Mixed-Phase TiO_2: Heterostructures and Electronic Properties. *J. Mol. Model.* **2014**, *20*, 2215.
(14) Kullgren, J.; Aradi, B. l.; Frauenheim, T.; Kavan, L.; Deák, P. Resolving the Controversy about the Band Alignment between Rutile and Anatase: The Role of OH^-/H^+ Adsorption. *J. Phys. Chem. C* **2015**, *119*, 21952−21958.
(15) Garcia, J. C.; Nolan, M.; Deskins, N. A. The Nature of Interfaces and Charge Trapping Sites in Photocatalytic Mixed-phase TiO_2 from First Principles Modeling. *J. Chem. Phys.* **2015**, *142*, 024708.
(16) Ju, M.-G.; Sun, G.; Wang, J.; Meng, Q.; Liang, W. Origin of High Photocatalytic Properties in the Mixed-Phase TiO_2: A First-Principles Theoretical Study. *ACS Appl. Mater. Interfaces* **2014**, *6*, 12885−12892.
(17) Nolan, M.; Deskins, N. A.; Schwartzenberg, K. C.; Gray, K. A. Local Interfacial Structure Influences Charge Localization in Titania Composites: Beyond the Band Alignment Paradigm. *J. Phys. Chem. C* **2016**, *120*, 1808−1815.
(18) Zhang, D.; Yang, M.; Dong, S. Electric-Dipole Effect of Defects on the Energy Band Alignment of Rutile and Anatase TiO_2. *Phys. Chem. Chem. Phys.* **2015**, *17*, 29079−29084.
(19) Li, L.; Yan, J.; Wang, T.; Zhao, Z. J.; Zhang, J.; Gong, J.; Guan, N. Sub-10 nm Rutile Titanium Dioxide Nanoparticles for Efficient Visible-Light-Driven Photocatalytic Hydrogen Production. *Nat. Commun.* **2015**, *6*, 5881.
(20) Lamiel Garcia, O.; Cuko, A.; Calatayud, M.; Illas, F.; Bromley, S. T. Predicting Size-dependent Emergence of Crystallinity in Nanomaterials: Titania Nanoclusters versus Nanocrystals. *Nanoscale* **2017**, *9*, 1049−1058.
(21) Lamiel-Garcia, O.; Ko, K. C.; Lee, J. Y.; Bromley, S. T.; Illas, F. When anatase nanoparticles become bulk-like: Properties of realistic TiO_2 nanoparticles in the 1 − 6 nm size range from all-electron relativistic density functional theory based calculations. *J. Chem. Theory Comput.* **2017**, *13*, 1785−1793.
(22) Blum, V.; Gehrke, R.; Hanke, F.; Havu, P.; Havu, V.; Ren, X.; Reuter, K.; Scheffler, M. Ab Initio Molecular Simulations with Numeric Atom-centered Orbitals. *Comput. Phys. Commun.* **2009**, *180*, 2175−2196.
(23) Wulff, G. Z. On the question of speed of growth and dissolution of crystal surfaces. *Z. Kristallogr.* **1901**, *34*, 449−530.
(24) Bromley, S. T.; Moreira, I. de P. R.; Neyman, K. M.; Illas, F. Approaching Nanoscale Oxides: Models and Theoretical Methods. *Chem. Soc. Rev.* **2009**, *38*, 2657−2670.
(25) Perdew, J. P.; Burke, K.; Ernzerhof, M. Generalized Gradient Approximation Made Simple. *Phys. Rev. Lett.* **1996**, *77*, 3865−3868.
(26) Ko, K. C.; Lamiel-García, O.; Lee, J. Y.; Illas, F. Performance of a Modified Hybrid Functional in the Simultaneous Description of Stoichiometric and Reduced TiO_2 polymorphs. *Phys. Chem. Chem. Phys.* **2016**, *18*, 12357−12367.
(27) Yu, H.; Li, J.; Loomis, R. A.; Wang, L.-W.; Buhro, W. E. Two- versus Three-Dimensional Quantum Confinement in Indium Phosphide Wires and Dots. *Nat. Mater.* **2003**, *2*, 517−520.
(28) Fu, H.; Zunger, A. InP Quantum Dots: Electronic Structure, Surface Effects, and the Redshifted Emission. *Phys. Rev. B: Condens. Matter Mater. Phys.* **1997**, *56*, 1496−1508.
(29) Brus, L. Electronic Wave-Functions in Semiconductor Clusters - Experiment and Theory. *J. Phys. Chem.* **1986**, *90*, 2555−2560.
(30) Rashid, M.; Tiwari, A. K.; Goss, J. P.; Rayson, M. J.; Briddon, P. R.; Horsfall, A. B. Surface-State Dependent Optical Properties of OH-, F-, and H-terminated 4H-SiC Quantum Dots. *Phys. Chem. Chem. Phys.* **2016**, *18*, 21676−21685.
(31) Xiong, G.; Shao, R.; Droubay, T. C.; Joly, A. G.; Beck, K. M.; Chambers, S. A.; Hess, W. P. Photoemission Electron Microscopy of TiO_2 Anatase Films Embedded with Rutile Nanocrystals. *Adv. Funct. Mater.* **2007**, *17*, 2133−2138.
(32) Kang, J.; Wu, F.; Li, S.; Xia, L.; Li, J. Calculating Band Alignment between Materials with Different Structures: The Case of Anatase and Rutile Titanium Dioxide. *J. Phys. Chem. C* **2012**, *116*, 20765−20768.
(33) Zhang, H.; Banfield, J. F. Thermodynamic Analysis of Phase Stability of Nanocrystalline Titania. *J. Mater. Chem.* **1998**, *8*, 2073−2076.
(34) Zhang, H.; Banfield, J. F. Structural Characteristics and Mechanical and Thermodynamic Properties of Nanocrystalline TiO_2. *Chem. Rev.* **2014**, *114*, 9613−9644.
(35) Ohno, T.; Tokieda, K.; Higashida, S.; Matsumura, M. Synergism Between Rutile and Anatase TiO_2 Particles in Photocatalytic Oxidation of Naphthalene. *Appl. Catal., A* **2003**, *244*, 383−391.
(36) Wahab, A. K.; Ould-Chikh, S.; Meyer, K.; Idriss, H. On the "Possible" Synergism of the Different Phases of TiO_2 in Photocatalysis for Hydrogen Production. *J. Catal.* **2017**, *352*, 657−671.

DOI: 10.1021/acs.jpclett.7b02474
J. Phys. Chem. Lett. 2017, 8, 5593−5598